INTECH
open science | open minds

OPEN ACCESS
ARTICLE

International Journal of Advanced Robotic Systems

Modelling and Analysis of Vibrations in a UAV Helicopter with a Vision System

Regular Paper

G. Nicolás Marichal Plasencia[1], María Tomás Rodríguez[2], Salvador Castillo Rivera[2] and Ángela Hernández López[1,*]

1 Departamento de Ing. de Sistemas y Automática, Arquitectura y Tecnología de Computadoras, Universidad de La Laguna, La Laguna, Tenerife, Spain
2 The Engineering and Mathematics Department. City University, London, United Kingdom
* Corresponding author E-mail: angela@isaatc.ull.es

Received 13 Jun 2012; Accepted 27 Aug 2012

DOI: 10.5772/52761

Abstract The analysis of the nature and damping of unwanted vibrations on Unmanned Aerial Vehicle (UAV) helicopters are important tasks when images from on-board vision systems are to be obtained. In this article, the authors model a UAV system, generate a range of vibrations originating in the main rotor and design a control methodology in order to damp these vibrations. The UAV is modelled using VehicleSim, the vibrations that appear on the fuselage are analysed to study their effects on the on-board vision system by using Simmechanics software. Following this, the authors present a control method based on an Adaptive Neuro-Fuzzy Inference System (ANFIS) to achieve satisfactory damping results over the vision system on board.

Keywords UAV, Vibrations, Vision System, Damping

1. Introduction

The modelling and generation of vibrations in UAV helicopters are complex issues due to difficulty in the identification of the various sources, for example: the main rotor, engine, and tail rotor are common sources of undesired vibrations. In addition to this, a thorough knowledge of the dynamical interaction existing between the main rotor and the fuselage is required in order to develop a complete and robust model that can help to control and damp these vibrations on an on-board vision system.

Several authors have previously studied and modelled UAV's systems. Mettler *et al.* described the process and results of the dynamic modelling of a model-scaled unmanned helicopter (Yamaha R-50 with 10ft rotor diameter) using system identification [1]. Del-Cerro presented several modelling techniques or strategies for dynamic modelling of helicopters such as: Godbole *et al.* [2], Mahony *et al.* [3], Gavrilets *et al.* [4], Metler *et al.* [5], La Civita *et al.* [6], and Castillo *et al.* [7]. They all proposed broad approaches performed in this field. Besides this, Del-Cerro described not only the modelling but also performed identification tasks. The proposed model was defined by using a hybrid (analytical and heuristic) algorithm [8]. El-Saadany *et al.* suggested that the need for using real vehicles in the control design cycle poses a high risk and is prohibitively expensive. As a consequence of this, a real-time simulation concept that employs cheap, practical, and rapid-to-build modular hardware, which can accurately simulate a real process in

the laboratory environment, is suggested. The authors integrated a nonlinear model for a small scale helicopter (Yamaha R-50) with sensors, servos, and wind models into a Simulink model [9]. On the other hand, Selier *et al.* dealt with the potential applications of unmanned helicopters in general as well as the current research and development activities in the Netherlands with the objective of realising an autonomous unmanned mini-helicopter [10].

The vibrations in a UAV helicopter have been dealt with and studied before; Cai *et al.* presented a comprehensive design methodology for constructing small-scale UAV helicopters. The systematic design procedure, which included hardware component selection, design and integration - as well as experimental evaluation - was used to construct a fully-functional UAV helicopter. In this work, the authors dealt with the main vibration sources in an UAV helicopter. The three sources were: rotation of the main rotor (30.8 Hz), tail rotor (143.4 Hz) and engine (260.5 Hz). These frequencies are estimated based on a governed motor speed of 1850rpm [11].

Dunbabin *et al.* presented a history of the design, challenges, constraints, and construction of an integrated isolated vision and sensor platform and landing gear for the CSIRO autonomous X-Cell helicopter. On the other hand, the authors state that a helicopter produces a unique and challenging environment in which all systems must operate correctly. Vibration sources can be mechanical, aerodynamic and from normal flight motion with broad amplitude and frequency spectrum. In this paper, the range of vibrations for autonomous helicopters is given as: main rotor speed (25 Hz), tail rotor speed (113 Hz), and engine speed (160) Hz [12].

In addition to this, Taha *et al.* put forward an avionics system, landing skid design, and vibration isolation. Analysis of helicopter vibration and stress on the landing skid based on flight data was given [13]. In the literature, we can also find documents dealing with the isolating components for UAV vibrations, i.e. the document from Micropilot. This work gives an overview of the vibration phenomenon as well as a starting point for experimental work [14].

From all these contributions, it can be seen that UAV helicopters, their modelling and vibration generated by the system itself hold great interest. In this study, the authors carry out the modelling of a UAV helicopter by use of VehicleSim software. The detailed modelling of the UAV dynamics provided in this paper allows for the analysis and study of vibration´s characteristics and nature. In addition, once the characterization of the vibrations has been completed, a control methodology based on an Adaptive Neuro-Fuzzy Inference System (ANFIS) has been used to show its effectiveness in damping the unwanted disturbances appearing on the vision system.

The paper is organized as follows: in section 2, the physical properties of the helicopter and model's parameters are presented. Section 3 briefly introduces VehicleSim, the software used for modeling this system. In section 4, vibration generation and analysis of their spectrum is carried out. The vision system is shown in section 5 and the proposed control algorithm is explained in section 6. Several results are shown in section 7 and finally section 8 contains the conclusions and suggestions for further research.

2. UAV Helicopter Dynamics and Model Description

Rotary-wing vehicles - usually helicopter-type - are composed of several subsystems. Of these, the most fundamental are the main rotor, the fuselage and the tail rotor. The role of the main rotor is to support the vehicle's weight, to create the lift forces that keep it suspended in the air, and to provide the control that allows following a prescribed trajectory in the various spatial directions by changing altitude and executing turns. The rotors of a helicopter, due to its rotating nature, are prone to introducing vibrations on the fuselage that may affect the vehicle's performance, the passengers' comfort and the accuracy of on-board measurement devices or vision systems (if any). The rotor of the model under consideration in this article is an articulated one and consists of two blades and two elevators equally spaced and connected to the central hub. The blades follow a uniform rotational motion imposed by the main rotor that rotates due to the engine's torque applied to the rotor's hub. The main rotor's rotational speed is represented by Ω (units are either radians per second or Hz).

(a) (b)

Figure 1. (a) Rotor's lag and feather hinges (b) Detail of the UAV model. Pictures taken at ULL Laboratories.

The blades can move in and out of the plane of the rotor disk; this is possible due to the presence of the hinges. The first hinge (located at a distance d from the rotor hub) provides the possibility of feathering (change of the angle of attack θ). This provides the needed lift force for the UAV to climb when the angle of feather is increased. On the other hand, if the feather angle is decreased, the

vehicle will descend accordingly. The simultaneous change of the blade's feather angle is known as collective control. This allows the rotorcraft to rise vertically. When the feather angle of each blade increases/decreases, at the same selected point on its circular pathway, on individual bases, at each revolution of the rotor, it is known as cyclic control and allows for turns in the space as it creates a differential lift force on the blades that induce a turning moment on the rotor. In the model under study in this paper there is a second hinge after the feathering one. This is the lag hinge, which provides stress-relief at the blade's root, reducing the bending moments and allowing the blade to rotate on the disk plane. The lagging angle, ξ, is considered to be positive when it is opposite to the direction of rotation of the rotor, as produced by the blade drag forces (see figure 2).

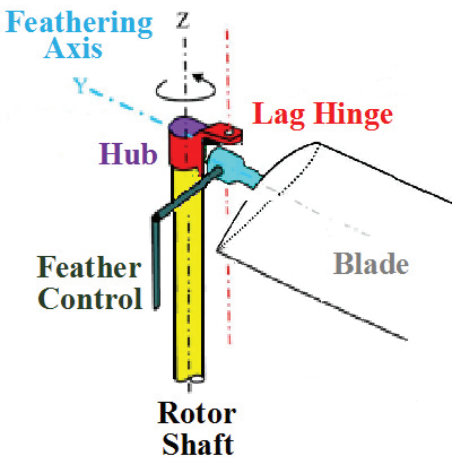

Figure 2. Schematic diagram of the main rotor's hub and hinges.

Finally, a flap hinge that allows the blade to rotate around an imaginary axis perpendicular to the rotor hub has been included in the computer model for simulation purposes (β represents the flap angle). In this way, the effect of the blade's flexibility at the root by allowing small motions in this direction is reproduced. It is convenient to note at this point that the flap hinge has not been included in figure 2 since it does not represent an element on the real rotor system. As was shown in figure 1, the real rotor system contains only feather and lag hinges.

On the other hand, the fuselage is the rotorcraft's main body section. It holds crew and passengers or cargo if large in size, or measurement devices, vision systems…etc., in the case of the UAV. Its degrees of freedom are the lateral and longitudinal translation in the horizontal plane (X-Y axis), vertical translation (Z axis) and rotation about these same axes corresponding to yaw ψ, pitch α and roll Φ degrees of freedom.

The tail rotor is mounted perpendicular to the main rotor and spins around the Y axis. It has two blades, which are equally spaced and connected to the fuselage by a hub. The blades follow a uniform rotational motion. The tail rotor's rotational speed is represented by Ω_t (radians per second or Hz).

The blades of the tail rotor are also connected to the tail hub by hinges. The first hinge (located at a distance d_t from the tail rotor hub) allows feathering motion. In addition to this, feather-flap dynamical coupling exists. This is a kinematic feedback of the flap angle into the blade's feather angle that is mathematically described as:

$$\Delta\theta = - k \beta \quad (1)$$

where θ is feather angle and k is the feather-flap coupling coefficient. It plays an important role in flight stability and the handling qualities of the vehicle, as well as aeroelastic stability of the blade. A flap hinge is also included in the tail rotor in order to allow the blade to rotate around an imaginary axis perpendicular to the tail rotor hub. Therefore, we can reproduce the effect of the blade's flexibility at the root by allowing motion in this direction. From (1) it is clear to see the effect of this dynamical coupling on the feather angle:

$$\Delta\theta = - \tan(\delta_3) \beta \quad (2)$$

δ_3 is usually a standard value chosen as 45º (0.785 rads). This dynamical coupling helps to reduce the transient and steady state flapping relative to the shaft.

The real model studied in this work is a Calibre 3 (see figure 1.b). Its parameters have been obtained either directly from the manufacturer's manual of use or by direct experimental measurements taken at ULL (La Laguna University) facilities.

The measured/obtained parameters are indicated in table 1. These are the values used for the simulations carried out in this work.

Parameters	Symbol	Value
Fuselage Mass	M_f	2.428 (kg)
Main Rotor Blade Mass	M_b	0.121 (kg)
Elevator Mass	M_{el}	0.041 (kg)
Tail Rotor Blade Mass	M_t	0.00441 (kg)
Vertical distance fuselage-main rotor	h	0.105 (m)
Main Rotor Blade length	l	0.55 (m)
Tail Rotor Blade length	l_t	0.08 (m)
Main Rotor Angular Speed	Ω	177.93 (rad/s)
Tail Rotor Angular Speed	Ω_t	889.65 (rad/s)

Table 1. Calibre 3 parameter's values.

The values indicated in table 1 will be introduced in the model developed in VehicleSim, the software tool used in this work. The next section contains the details of the modeling process.

3. Modelling Tool: VehicleSim

VehicleSim is multibody modelling software. The system has been used over a wide range of mechanical dynamic problems, mainly in connection with vehicle dynamics ([16], [17], [18]) and it has provided the basis for commercial simulation codes such as TruckSim, CarSim and BikeSim [15]. The syntactic rules of VehicleSim are straightforward. The output from VehicleSim can take one of several forms: (a) a Rich Text Format file containing the symbolic equations of motion of the system described; (b) a"C" language simulation program with appropriate data files containing parameter values and simulation run control parameters or (c) linear state-space equations in a MATLAB "M-file" format that contains symbolic state-space *A*, *B*, *C*, *D* matrices that can be used for linear analysis.

Once the model has been built, it becomes independent of VehicleSim and can be executed at any time. The multibody basis of VehicleSim is Kane's equations, which is an alternative statement of the Newton- Euler-Jordan (virtual power) principle. It has been proven that with this method, fewer operations are needed to derive equations of motion, compared with the well known Lagrange's energy-based method that can only accommodate holonomic constraints and introduces many cancelling terms in the computations.

4. Vibration and Analysis

The complete dynamical helicopter model was implemented as described in section 2 using the parameters indicated in Table 1. It is assumed that the engine regime is 1700 rpm (revolution per minute). The fuselage has 6 degrees of freedom: longitudinal, lateral and vertical along the axes X, Y, Z respectively and the corresponding rotations about these same axes. The acceleration of gravity in these simulations is neglected (VehicleSim allows for switching off the gravity) as the purpose of these simulations is to analyse the forces and accelerations that appear as a result of interactions and couplings between the various UAV components only.

In order to study the characteristics of the vibrations appearing in the fuselage due to the main rotor only, a simulation is carried out where the main rotor has an angular velocity of Ω=177.9 rad/s, and the tail rotor speed is Ω_t=0rad/s. As the main objective at this stage is vibration generation, a mass imbalance can be introduced artificially in order to produce vibrations, i.e. the mass of the second blade (main rotor) is set to be the double of the other blade's masses (M_{b2}=0.282kg). The vibrations that appear will be transmitted to the fuselage.

The vibrations appearing along the fuselage's X and Z axis are shown for VehicleSim simulations carried out for a duration of 5 seconds. The output of the simulation (time history of the position, velocities and accelerations on the fuselage) were obtained, stored in the workspace and analysed using a FFT (Fast Fourier Transform) Matlab algorithm. It was found that the main frequency component of the spectrum of vibration appearing on the fuselage's X-axis is f=28.32Hz, (177.93rad/s) (see figure 3).

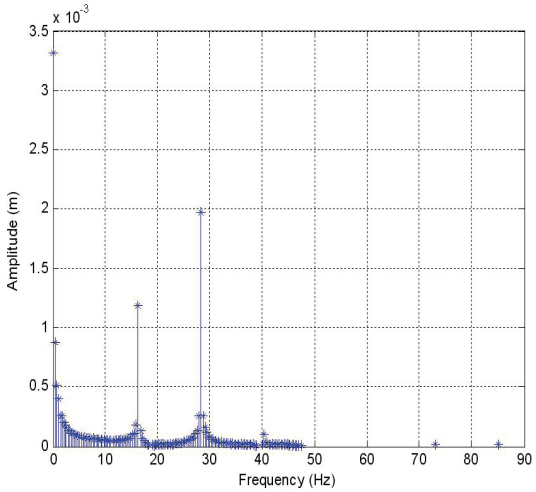

Figure 3. Frequency and Amplitude of vibrations appearing on the fuselage's longitudinal axis (X).

It is evident that the main peak of frequencies is around 28.32Hz. This is caused by the main rotors blade's mass imbalance. In fact these results follow theoretical predictions [11], [12].

In the same way, if the spectrum of vibrations appearing on the fuselage's vertical direction (Z axis) is analysed, frequencies of 16.36Hz (102.79rad/s) and 28.32Hz (177.93rad/s) appear as major contributors of the spectrum (see figure 4).

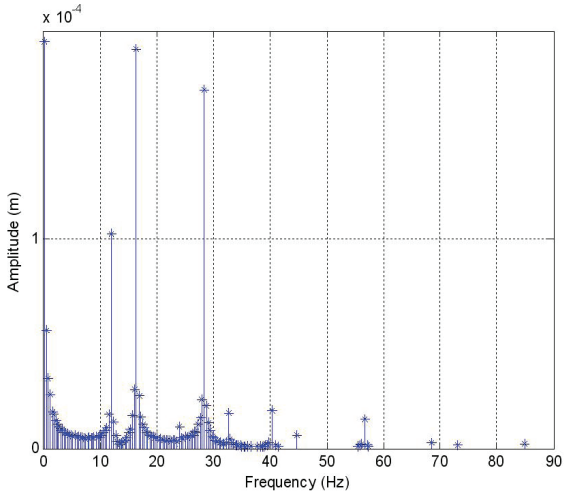

Figure 4. Frequency and Amplitude of vibrations appearing on the fuselage's vertical axis (Z).

Two peaks of frequencies appear and their amplitudes are of similar ranges. The source of the vibration

characterised by the dominant frequency is the steady load of the system, i.e. the tail rotor and the fuselage shapes and configurations. The secondary peak in this case is caused by the main rotor and its mass imbalance, as it was in the case of the longitudinal vibrations (figure 3). The ranges of peak frequencies detected in these simulations will be used later in the following sections, in order to design a control algorithm that will isolate the vision system from these unwanted disturbances at the indicated frequencies.

5. Vision System

Studying the effect of the vibrations produced by the helicopter on an on-board vision system is one of the aims of this work. With the purpose of analysing the behaviour of a camera if it is subjected to different disturbances, a vision system consists of a dynamic platform SPT 200 SERVICITY and a camera, all modelled in Simulink/Simmechanics [19]. This platform has three bodies separated by servomotors, providing two degrees of freedom to the system, such as yaw and pitch angles. The first body is the base that is fixed to the fuselage and the camera is placed over the third body as can be seen in Figure (5).

Figure 5. Vision system consisting of the dynamic platform with the camera.

The Inertia matrices and other geometric parameters of each body were calculated and subsequently introduced in the simulation platform. The simulation developed in Simulink/Simmechanics includes the camera, the dynamic platform modelled with elements that simulate its flexibility, as well as the servomotors and a PID controller for each joint. Furthermore, two input blocks for the vibration are put in the simulation environment since the aim of this modelling is to analyse the camera undesired movement if the fuselage is transmitting vibrations. Specifically, the effects of the helicopter vibration of the gravity axis (Y) and a perpendicular axis (Z) are studied.

6. Control Algorithm

The chosen isolation method used to reduce the vibration suffered by the camera is a spring-damper system with a variable damping value C(t). The fact that the damping value is time-dependant makes possible an adaptive control with the capability of changing according to the vibration received from the helicopter. The change of the damping variable is provided by an intelligent system designed to give the most adequate C value for each case. In this work, the parameters to be considered are the vibration frequencies. In other words, the adaptive control system analyses the frequencies of the disturbance produced by the helicopter in two axes and decides the best C value for each time interval.

Due to these dependencies, it is necessary to create a table where the more suitable damping value is provided according to the frequencies f_y and f_z. From now on, this table will be known as "reference table". In order to fill this table, an iterative process is carried out whereby the C value is modified for each combination of f_y and f_z. A criterion function was defined with the purpose of deciding the most appropriate damping value for each case. This function is such that the camera displacement around the equilibrium position was as low as possible. Particularly, the standard deviation evaluates these undesired camera movements. In this way, the damping value that minimises the camera vibration for each combination of frequencies is chosen. Therefore, once the iterative process has been concluded, the reference table is built as a result of the minimization process of the criterion function. It allows finding the most suitable C value corresponding to a particular combination of the frequencies f_y and f_z.

The next step is to design an intelligent system capable of providing the C value for each case based on the reference table. Because of this, a method based on training is necessary. Therefore an artificially intelligent system is chosen. An Adaptive Neuro-Fuzzy Inference System (ANFIS) [20] has been used. This method has neuro-adaptative learning, that is to say, it works similarly to neural networks, using a given input/output data set. Specifically, in this work the input data set is [f_y f_z] and its corresponding output set is [C].

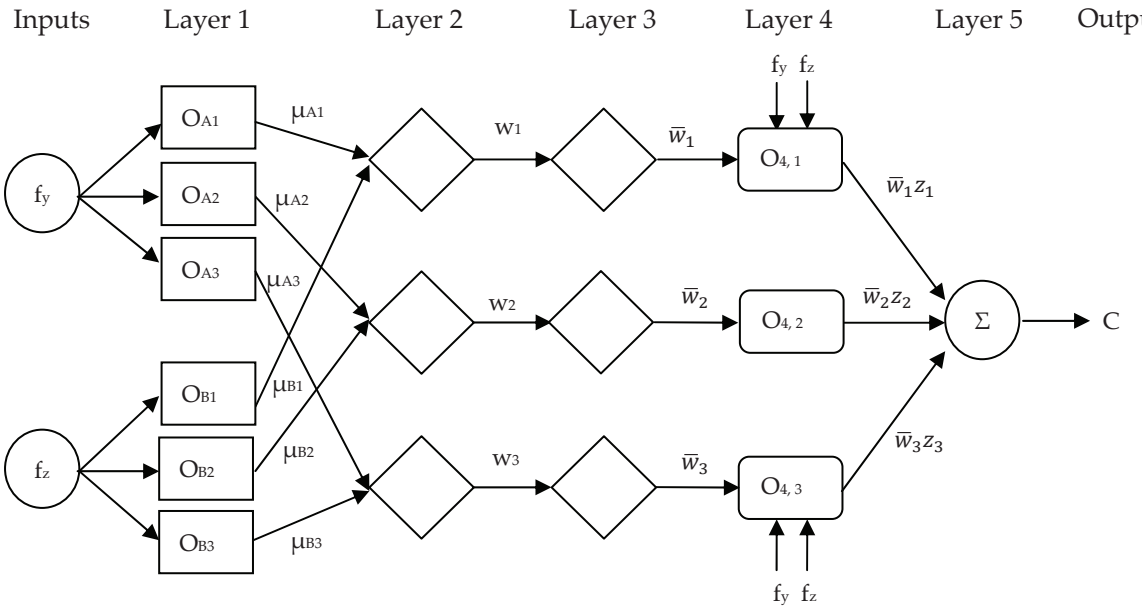

Figure 6. Architecture of the used Adaptive Neuro-Fuzzy Inference System.

The ANFIS architecture is shown in Figure 6. It consists of five layers with two inputs, each one with three membership functions μ_{Ai} y μ_{Bi} (i=1, 2, 3), respectively, and an output C.

The first step is to choose the number and type the membership functions (MF) for each input and to determine their membership degree values. In this way, two inputs and three Generalized Bell MF were chosen for each input. In the first layer each node has an output defined as:

$$0_{A,i} = \mu_{Ai}(f_y) \tag{3}$$

$$0_{B,i} = \mu_{Bi}(f_z),\ i = 1,2,3 \tag{4}$$

In the second layer the fuzzy operator is applied, therefore the input signals are multiplied and the result represents the weight of each rule.

$$w_i = \mu_{Ai}(f_y)\mu_{Bi}(f_z),\ i = 1,2,3 \tag{5}$$

The Implication method is applied in the third layer and the output of each node corresponds to the standard weights, which is a number between 0 and 1.

$$\bar{w}_i = \frac{w_i}{\sum_{i=1}^{n} w_i},\ \text{i= 1,…n} \tag{6}$$

The aggregation is presented in the fourth layer and consists of the fuzzy sets that represent the outputs of each rule combined into a single fuzzy set.

$$O_{4,i} = \bar{w}_i z_i\ i = 1,2,3 \tag{7}$$

Where z_i corresponds to three fuzzy if-then rules of Takagi-Sugeno type which are:

If f_y is μ_{A1} and f_z is μ_{B1} then $z_1 = p_1 f_y + q_1 f_z + r_1$ (8a)

If f_y is μ_{A2} and f_z is μ_{B2} then $z_2 = p_2 f_y + q_2 f_z + r_2$ (8b)

If f_y is μ_{A3} and f_z is μ_{B3} then $z_3 = p_3 f_y + q_3 f_z + r_3$ (8c)

Where p_i, q_i, r_i are the consequent parameters.

Finally, the fifth layer applies the *defuzzification* process. That is, it adds all outputs of the fourth layer and gives as output a real number corresponding to damping value. In this paper, this process is done by a weighted average as follows:

$$C = \frac{\sum_{i=1}^{N} \bar{w}_i Z_i}{\sum_{i=1}^{N} \bar{w}_i} \tag{9}$$

Where C is the damping value given as system output, z_i is the output level of each rule; w_i is the weight of each rule weighted and N the total number of nodes at layer 3.

To summarise, the process of building an ANFIS model has three phases: collecting the input/output data set that will be used by ANFIS for training, the creation of a Fuzzy Inference System as an initial structure [21, 22] and finally the application of a learning algorithm (backpropagation gradient).

The reference table, obtained with the iterative process explained previously, is the necessary data set in order to start the training phase. This input/output set is divided into two groups, where eighty percent of them are used in the ANFIS training and the remaining twenty percent is kept back in order to test if the system has achieved the adequate degree of generalisation.

Once the ANFIS system has been trained, it is included in the simulation environment as a Simulink block. As this block needs the frequencies f_y and f_z as inputs, a method that calculates them from the vibration signals is required. A FFT block is added between the vibration produced by the helicopter and the ANFIS in the Y and Z axis. These blocks are in charge of obtaining the spectral composition of the signal on each axe applying the Fast Fourier Transform at intervals of 0.5 seconds. When the ANFIS analyses the input frequencies, it provides the best C value every 0.5s. In this way, the damping value provided is introduced into the semi-active control system that is placed between the fuselage and the base of the dynamic platform.

7. Results

With the semi-active isolation system and the ANFIS controller added to the simulation environment, the vibrations from the helicopter are introduced by two blocks: one for each axe. The following step is to analyse the camera behaviour subjected to these vibrations and to test the validity of the proposed control technique. The vibrations produced by the fuselage over the X axe and Z axe are shown in Figures 7 and 8 respectively. It is necessary to point out that these vibrations are obtained by the helicopter simulation platform.

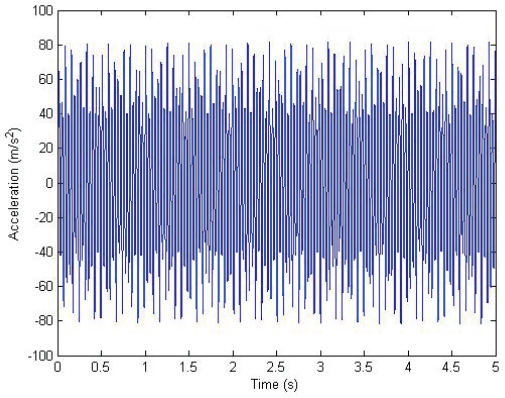

Figure 7. Vibration from fuselage over the X axe.

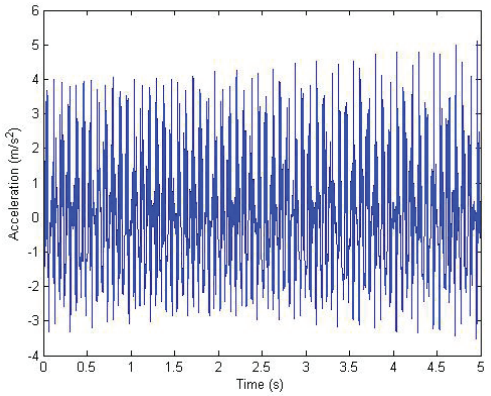

Figure 8. Fuselage vibration over the Z axe.

Once the signals have been introduced in the simulation, the next step is to analyse the camera behaviour. Firstly, we measure the camera movement under the influence of the vibrations when there is no isolation system fitted. Figure 9 shows this behaviour over the gravity axe Z. As could be observed, the camera suffers an abrupt movement during the first half second reaching 5mm of amplitude and after this, the camera maintains a residual vibration of about 0.5mm. Observing this result, the need for including an isolation system to reduce these vibrations and to achieve a more stable vision system is clear.

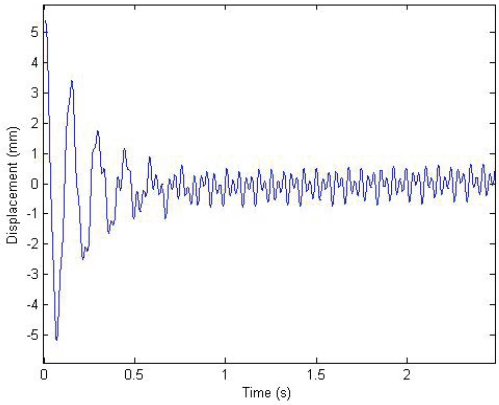

Figure 9. Camera vibration over the Z axe without isolation system.

The proposed method based on ANFIS was used taking into account the vibrations shown in Figures 7 and 8. As was explained previously, the system calculates the frequencies on each axe at each 0.5s and depending on these values, the ANFIS gives the most adequate damping value C. In Figure 10 we observe the dominant frequencies obtained by the FFT block in the Z axe.

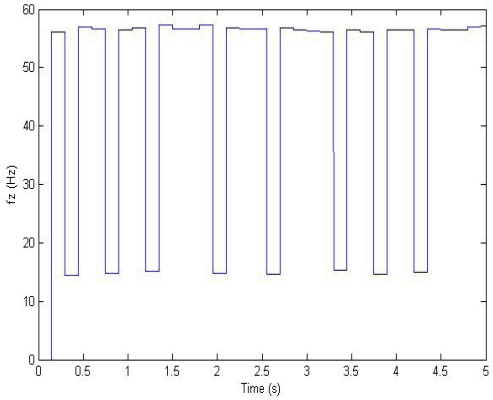

Figure 10. Dominant frequencies in Z axe.

With the purpose of checking the efficiency of the proposed method, the obtained results are compared with a passive damping case. That is to say, the vibration suffered by the camera with the semi-active method based on ANFIS and with a passive technique. This

comparison is shown in Figure 11. It is observed that the method with the damping value constant shows worse behaviour during the first half second than the C variable technique. The ANFIS method reduces the undesirable movement of the camera in the first ten seconds. After elapsing 1 second, both techniques are stabilised and keep the camera vibration near zero.

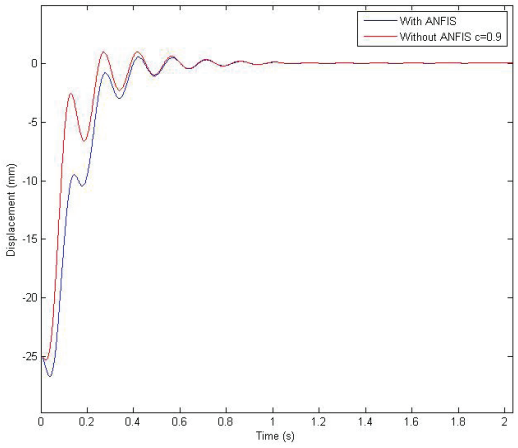

Figure 11. Comparison of the camera movement with the proposed ANFIS technique and with passive method.

8. Conclusion

A UAV helicopter was modelled in VehicleSim and used to obtain the vibration produced by the main rotor on its fuselage. An on-board vision system fitted on the fuselage will suffer the effects of these unwanted vibrations unless a control system is applied in order to damp those. The results presented here allow knowing the level of vibration that will affect the vision system. The knowledge of the predominant frequencies allows the training of an intelligent control that will adapt itself depending on the values of these frequencies and will provide the adequate damping value for each situation.

The trained isolation device is introduced into the Simulink platform with the vision system composed by the dynamic platform and the camera. Therefore, when the vibrations produced on the fuselage are introduced into the simulation, it is possible to observe and to analyse the camera behaviour under the effect of these vibrations.

The simulations carried out show that the proposed method based on a semi-active device with the damping value provided by an ANFIS improves the camera behaviour. This improvement allows clearer images to be obtained.

9. Acknowledgements

This work has been supported by the Spanish Government project DPI2010-20751-C02-02 of Ministerio de Ciencia e Innovación and by the grant of the Agencia Canaria de Investigación, Innovación y Sociedad de la Información del Gobierno de Canarias, cofinanced with the European Social fund.

10. References

[1] B. Mettler, T. Kanade, M.B. Tischler. "System Identification Modelling of a Model-Scale Helicopter". CMU-RI-TR-00-03

[2] D.N. Godbole et al. "Active Multi-Model Control for Dynamic maneuver Optimization of Unmanned Air Vehicles." (2000). Proceedings of the 2000 IEEE International conference on Robotics and Automation. San Francisco, CA. April.

[3] R. Mahony and R. Lozano. "Control for an Autonomous helicopter in Hover Manoeuvres". (2000). Exact Path Tracking. Proceedings of the 2000 IEEE International Conference on Robotics & Automation. San Francisco, CA. APRIL. P. 1245-1250

[4] V. Gavrilets, E. Frazzoli, B. Mettler. "Aggressive Maneuvering of Small Autonomous Helicopters: A. Human Centered Approach" (2001). The International Journal of Robotics Research. Vol 20, Nº 10, October. pp 795-807

[5] B.F. Mettler, M.B. Tischler, T. Kanade. "System Identification Modeling of a Model-Scale Helicopter". (2000). T. Journal of the American Helicopter Society. 47/1: p. 50-63

[6] M. La Civita, W. Messner, T. Kanade. "Modeling of Small-Scale Helicopters with Integrated First-Principles and System-Identification Techniques". (2002). American Helicopter Society 58th Annual Forum, Montreal, Canada, June 11-13

[7] P. Castillo, R. Lozano, A. Dzul. "Modeling and Control of Mini-Flying Machines". 2005. Springer Verlag London Limited. ISBN: 1852339578

[8] J. Del-Cerro. A. Barrientos, A. Martinez. "Modeling and Control Prototyping of Unmanned Helicopters". Universidad Politécnica de Madrid. Robotics and Cybernetics Group. Spain

[9] A. El-Saadany, A. Medhat, Y. Z. Elhalwagy. "Flight Simulation Model for Small Scaled Rotor Craft-Based UAV". 2009. 13th International Conference on Aerospace Sciences & Aviation Technology. Asat-13. May 26-28. Paper: Asat-13-CT-31

[10] M. Selier and G. Voorsluijs. "Future Surveillance Using Autonomous Unmanned Helicopters". 2003. American Institute of Aeronautics and Astronautics.

[11] G. Cai, L. Feng, B.M. Chen, T.H. Lee. "Systematic Design Methodology and Construction of UAV Helicopters". 2008. Mechatronics, 18, 545-558

[12] M. Dunbabin, S. Brosnan, J. Roberts, P. Coke. "Vibration Isolation for Autonomous Helicopter Flight". 2004. International Conference on Robotics & Automation. 0-7803-8232-3/04, IEEE. New Orleans, April

[13] Z. Taha, K.C. Yap, Y. Tang. "Avionics Box for a Small Unmanned Helicopter". 2008. Proceedings of the 9th Asia Pacific Industrial Engineering & Management Systems Conference. Indonesia. December 3rd -5th

[14] Micro Pilot. Newsletter. World Leader. Miniature UAV Autopilots. ISO9001:2000

[15] Available http://www.carsim.com

[16] M. W. Sayers (1999) Vehicle models for RTS applications. Vehicle System Dynamics 32(4-5): 421-438

[17] R.S. Sharp, Evangelou S and Limebeer DJN, Multibody aspects of motorcycle modeling with special reference to Autosim, Advances in Computational Multibody Systems, J. G. Ambrósio (Ed.), Springer- Verlag, Dordrecht, The Netherlands, 2005, 45-68

[18] M.Tomás-Rodríguez, R Sharp, Automated Modeling of Rotorcraft Dynamics with Special Reference to Autosim, Automation Science and Engineering, 2007. CASE 2007. IEEE International Conference, 2007

[19] Available:
http://www.mathworks.com/products/simulink/

[20] J.R. Jang. ANFIS: Adaptive-network-based fuzzy inference system. IEEE Trans. Syst. Man Cybern. 1993, 23, 665-685

[21] M. Guijarro, G. Pajares. On combining classifiers through a fuzzy Multicriteria Decision Making Approach: applied to natural textured images. Expert Syst. Appl. 2009, 36, 7262-7269.

[22] L.A Zadeh. Knowledge representation in fuzzy logic. IEEE Trans. Knowl. Data Engin. 1989, 1, 89-100.